Mechanism of NO-Induced Oxidation of Myoglobin and Hemoglobin†

Raymund F. Eich,‡ Tiansheng Li,‡,|| Douglas D. Lemon,§ Daniel H. Doherty,§ Shawn R. Curry,§ Jacqueline F. Aitken,§ Antony J. Mathews,§ Kenneth A. Johnson,‡,⊥ Robert D. Smith,‡ George N. Phillips, Jr.,‡ and John S. Olson*,‡

Department of Biochemistry and Cell Biology and the W. M. Keck Center for Computational Biology, Rice University, 6100 Main Street, Houston, Texas 77005-1892, and Somatogen, Inc., 2545 Central Avenue, Boulder, Colorado 80301

Received February 23, 1996; Revised Manuscript Received April 22, 1996⊗

ABSTRACT: Nitric oxide (NO) has been implicated as mediator in a variety of physiological functions, including neurotransmission, platelet aggregation, macrophage function, and vasodilation. The consumption of NO by extracellular hemoglobin and subsequent vasoconstriction have been suggested to be the cause of the mild hypertensive events reported during *in vivo* trials of hemoglobin-based O_2 carriers. The depletion of NO from endothelial cells is most likely due to the oxidative reaction of NO with oxyhemoglobin in arterioles and surrounding tissue. In order to determine the mechanism of this key reaction, we have measured the kinetics of NO-induced oxidation of a variety of different recombinant sperm whale myoglobins (Mb) and human hemoglobins (Hb). The observed rates depend linearly on [NO] but show no dependence on $[O_2]$. The bimolecular rate constants for NO-induced oxidation of MbO_2 and HbO_2 are large ($k'_{ox,NO} = 30-50\ \mu M^{-1}\ s^{-1}$ for the wild-type proteins) and similar to those for simple nitric oxide binding to deoxygenated Mb and Hb. Both reversible NO binding and NO-induced oxidation occur in two steps: (1) bimolecular entry of nitric oxide into the distal portion of the heme pocket and (2) rapid reaction of noncovalently bound nitric oxide with the iron atom to produce $Fe^{2+}-N{=}O$ or with $Fe^{2+}-O-O^{\delta-}$ to produce $Fe^{3+}-OH_2$ and nitrate. Both the oxidation and binding rate constants for sperm whale Mb were increased when His(E7) was replaced by aliphatic residues. These mutants lack polar interactions in the distal pocket which normally hinder NO entry into the protein. Decreasing the volume of the distal pocket by replacing Leu(B10) and Val(E11) with aromatic amino acids markedly inhibits NO-induced oxidation of MbO_2. The latter results provide a protein engineering strategy for reducing hypertensive events caused by extracellular hemoglobin-based O_2 carriers. This approach has been explored by examining the effects of Phe(B10) and Phe(E11) substitutions on the rates of NO-induced oxidation of the α and β subunits in recombinant human hemoglobin.

Nitric oxide (NO) is a ubiquitous signal transduction molecule which freely diffuses across cell membranes but has a relatively short half-life on the order of seconds to minutes due to its reaction with molecular oxygen (Ignarro, 1990; Snyder & Bredt, 1992; Kharitonov et al., 1994). One important function of NO is the mediation of smooth muscle relaxation. In response to circulatory signals, nitric oxide synthase can be stimulated to produce high levels of NO (up to 5 μM) in arterial endothelial cells (Moncada et al., 1991). The gas then diffuses into adjacent smooth muscle cells, activates guanylyl cyclase, and triggers a cascade of metabolic events that culminate in smooth muscle relaxation.

Hypertensive events are often seen during the administration of extracellular hemoglobin-based O_2 carriers and have been attributed to disruption of the NO signaling pathway [Hess et al., 1993; Lee et al., 1995; Lieberthal et al., 1987; reviewed by Vandegriff (1992, 1995)]. Most recent evidence suggests that this effect is due to reaction of NO with hemoglobin that has been taken up by endothelial cells or entered into the space between these cells and smooth muscle tissue. NO binding to ferrous deoxyhemoglobin (Hb) has been proposed to be the main mechanism for NO depletion [reviewed in Vandegriff (1992, 1995)]. Deoxyhemoglobin has an extremely high affinity for NO ($K_{dissociation} \approx 4$ pM), and although its concentration relative to HbO_2 is small in the vicinity of arterioles, the absolute amount ($\sim$500 μM) is still sufficient to bind NO produced by endothelial cells. Kosaka et al. (1994) and others have shown that stimulation of NO production in endothelial cells by cytokines produces significant amounts of HbNO *in vivo*.

Binding to methemoglobin (Hb^+) and oxidation/reduction cycles of free hemin have also been proposed as causes of NO consumption, particularly in the spaces between the endothelium and smooth muscle (Alayash et al., 1993; Alayash & Cashon, 1994). However, Hb^+ is normally present in small amounts in most extracellular hemoglobin preparations ($\leq$5−20%), and the affinity of NO for Hb^+ is too low ($K_{dissociation} \approx 5 \times 10^{-4}$ M) to allow appreciable binding at physiological concentrations (i.e. [NO] = 10^{-12}

† Supported by United States Public Health Service Grants AR 40252 (G.N.P.), GM 35649 (J.S.O.), and HL 47020 (J.S.O.), Grants C-1142 (G.N.P.) and C-612 (J.S.O.) from the Robert A. Welch Foundation, and the W. M. Keck Foundation. R.F.E. is a recipient of a predoctoral fellowship from the National Institutes of Health Training Grant GM08280.

* Corresponding author: John S. Olson, Department of Biochemistry and Cell Biology, Rice University, MS 140, 6100 Main Street, Houston, TX 77005-1892, Office phone: 1-713-527-4762. Laboratory phone: 1-713-527-4861. Fax number: 1-713-285-5154. E-mail: olson@rice.edu.

‡ Rice University.

§ Somatogen, Inc.

|| Current address: Protein Chemistry Department, AMGEN, Inc., Thousand Oaks, CA.

⊥ Current address: Department of Biochemistry, Baylor College of Medicine, Houston, TX.

⊗ Abstract published in *Advance ACS Abstracts,* May 15, 1996.

S0006-2960(96)00442-4 CCC: $12.00

to 10^{-6} M). In addition, the rates of hemin dissociation from methemoglobin are fairly slow ($\sim 0.5-2.0$ h^{-1}; Hargrove et al., 1994), whereas the vasoconstriction response occurs quickly.

In our view, the reaction of NO with extracellular oxyhemoglobin probably accounts for most of the NO depletion responsible for vasoconstriction. HbO_2 is the predominant form in arterial blood, and its reaction with NO is thought to be as rapid as that for NO binding to deoxy-Hb (Doyle & Hoekstra, 1981). Surprisingly, the mechanism of NO-induced oxidation of HbO_2 is poorly understood despite its physiological importance and its use as an assay of NO production *in vivo* and in isolated NO synthase preparations (Ignarro, 1990; Moncada et al., 1991; Marletta, 1993; Hurshman & Marletta, 1995). Doyle and Hoekstra (1981) showed that the products of the reaction of MbO_2 or HbO_2 with NO are exclusively met-Mb or met-Hb and NO_3^-. Because no ferrous HbNO or MbNO was observed, the rate of direct oxidation must be at least 20-fold faster than the rate of O_2 displacement by NO (Doyle & Hoekstra, 1981). There was only a small effect of oxygen concentration on the amounts and ratio of reaction products, implying that the rate of NO reaction with free O_2 is much smaller than that with oxygen bound to the heme group. The latter result also indicated that NO is the oxidizing species and not nitrite or any other product of aerobic oxidation.

A number of key problems were left unresolved, including determination of the absolute value of the rate constant for NO-induced oxidation and the mechanism of the oxidative process. To address these issues, we measured the kinetics of NO-induced oxidation using rapid mixing techniques. We also sought to identify structural features which regulate the rate of the reaction. These goals were achieved by examining the effects of amino acid substitutions at the His(E7), Leu(B10), and Val(E11) positions in recombinant sperm whale myoglobin and at the Leu(B10) and Val(E11) positions in recombinant human hemoglobin. The results have led to a protein-engineering strategy for selectively inhibiting NO-induced oxidation of extracellular O_2 carriers. Our goal is to design recombinant hemoglobin molecules that do not interfere with vasodilation, even if they enter the endothelium and surrounding tissues.

MATERIALS AND METHODS

Myoglobin and Hemoglobin Mutagenesis. B10, E7, and E11 mutants of sperm whale Mb were constructed, expressed, and purified as described previously by Carver et al. (1992), Springer et al. (1989), and Egeberg et al. (1990), respectively, using the recombinant gene constructed by Springer and Sligar (1987). The protein expressed from this gene has been designated wild-type since its ligand binding properties are identical to those of native sperm whale myoglobin [see Rohlfs et al. (1990)]. However, it contains an "extra" N-terminal Met and an Asp122 to Asn substitution.

Recombinant human hemoglobin was prepared using a derivative of plasmid pSGE0.0E4 (Hoffman et al., 1990). A single operon directs expression of one α and one β globin cistron under control of the *tac* promoter. In each cistron, the N-terminal Val codon is replaced by the translational initiator codon for Met. The α(V1M) β(V1M) genes serve as the background for mutagenesis studies, and the resulting hemoglobin is designated rHb(0.0) and serves as the "wild-type" control. Mutations were introduced at the α and β B10 and E11 positions by site-directed mutagenesis using PCR (Innis et al., 1990). PCR-mutagenized DNA fragments were cloned into the expression vector ,and mutant sequences were confirmed by DNA sequencing.

Table 1: Comparison of the Bimolecular Rate Constants for NO-Induced Oxidation with Those for NO Binding to Ferrous (Fe^{2+}) and Ferric (Fe^{3+}) Leu(B10), His(E7), and Val(E11) Mutants of Recombinant Sperm Whale Myoglobin[a]

Mb	$k'_{ox,NO}$ (μM^{-1} s^{-1})	$k'_{NO}(Fe^{2+})$ (μM^{-1} s^{-1})	$k'_{NO}(Fe^{3+})$ (μM^{-1} s^{-1})
wild-type	34	22	0.070
Val29(B10)	38	28	0.250
Phe29(B10)	8.1	27	0.055
Trp29(B10)	3.2	1.6	0.043
Gln64(E7)	160	43	8.2
Ala64(E7)	140	150	46
Val64(E7)	260	270	160
Leu64(E7)	210	190	50
Phe64(E7)	60	57	33
Leu68(E11)	24	46	0.069
Ile68(E11)	33	26	0.260
Phe68(E11)	9.4	1.9	0.028
Trp68(E11)	4.1	0.62	0.010

[a] All rates were measured at 20 °C in 0.1 M potassium phosphate and 0.3 mM EDTA (pH 7.0). Our wild-type, recombinant protein has ligand binding properties identical to those of native sperm whale myoglobin even though it contains an extra N-terminal Met and an Asp122 to Asn substitution [see Rohlfs et al. (1990)].

Early preparations of the recombinant hemoglobins were purified as described by Looker et al. (1992) employing Fast Flow Sepharose S and Q columns (Pharmacia). Later preparations employed a Fast Flow Zn Chelating Sepharose (Pharmacia) column to "capture" hemoglobin on the resin and wash away most of the contaminating *Escherichia coli* proteins. Normal O_2 equilibrium curves were obtained for rHb(0.0), and simple accelerating time courses for CO binding to the deoxy form of this protein were observed with $k'_{CO} \approx 2 \times 10^5$ M^{-1} s^{-1} [see Looker et al. (1992) and Komiyama et al. (1991)].

NO Solutions. Stock solutions of nitric oxide were made by injecting anaerobic buffer into a gas-tight tonometer flushed with 1 atm of NO that had been pretreated to remove acids (NO_2). After equilibration of the buffer with NO gas, aliquots of this stock solution ($\sim$ 2 mM) were injected into syringes containing anaerobic buffer to achieve the desired dilution. The stock NO solution was standardized by measuring pseudo first-order rates of NO binding to native sperm whale metmyoglobin and then calculating [NO] using independently determined values of $k'_{NO}(Fe^{+3})$ and $k_{NO}(Fe^{3+})$ (0.070 μM^{-1} s^{-1} and 15 s^{-1}, respectively; Table 1; Sharma et al., 1983, 1987).

Kinetics Measurements. The buffers used were 0.1 M potassium phosphate and 0.3 mM EDTA (pH 7.0) for the myoglobin reactions and 0.1 M sodium phosphate (pH 7.4) for the hemoglobin reactions. All rate constants were calculated from multiple determinations at 20 °C. Rate constants for NO association to ferrous Mb, $k'_{NO}(Fe^{+2})$, were measured using laser flash photolysis techniques as described by Gibson et al. (1992). The only exception was $k'_{NO}(Fe^{+2})$ for the V68W mutant which has a quantum yield that is effectively zero. The association rate constant for NO binding to the ferrous form of Trp68 Mb is very slow and

easily measured by conventional rapid mixing techniques. Absorbance time courses for NO binding to met-Mb were measured at 419 nm using a Gibson−Durrum stopped-flow spectrometer. Association rate constants, $k'_{NO}(Fe^{+3})$, were obtained from the slopes of plots of the observed pseudo first-order rate constants versus [NO].

Time courses for the reaction of NO with MbO_2 and HbO_2 were measured by stopped-flow rapid mixing techniques using the Gibson−Durrum stopped-flow device at Rice University or the Applied Photophysics stopped-flow device at Somatogen. Met-Mb and met-Hb formation were monitored as absorbance increases at 409 and 402 nm, respectively. Due to the extremely large values of $k'_{ox,NO}$ for wild-type and the E7 mutants, NO concentrations had to be kept low (1−25 μM) to prevent the reaction from going to completion during the dead time of the instrument (2−3 ms). As a result, very low protein concentrations (~0.2−1 μM) were required to maintain pseudo first-order conditions, small absorbance changes were observed, and averaging of 8−12 traces was necessary to enhance the signal to noise ratio.

The presence of free O_2 in the reaction mixture has no substantive impact on $[NO]_{free}$ during the time course of NO-induced oxidation. NO does react with free O_2; however, the half-time for this inorganic reaction is on the order of seconds to minutes at low nitric oxide concentrations due to a second-order dependence on $[NO]_{free}$ (Kharitonov et al., 1994). Under the same conditions, the oxidation of MbO_2 and HbO_2 by NO is complete within 30−200 ms (Figures 1 and 4).

X-ray Crystallography. The structures of the ethyl isocyanide (EtNC) complexes of the α and β subunits of native human hemoglobin were reported by Johnson (1993), and the structure of the EtNC complex of recombinant wild-type sperm whale myoglobin was determined for this work. The crystal was grown in the *P*6 form using 2.2−2.6 M ammonium sulfate, 20 mM Tris, and 1 mM EDTA, as described by Phillips et al. (1990). The unit cell parameters were $a = b = 91.6$ Å, $c = 46.0$ Å, $\alpha = \beta = 90°$, and $\gamma = 120°$. Diffraction data for the MbEtNC complex were collected to 1.7 Å resolution on a Rigaku R-axis IIC and processed using Rigaku-supplied software. The number of unique reflections was 18 453 with 76.0% completeness. Starting models for the refinement of the MbEtNC structures were generated from the structure of wild-type MbCO (Quillin et al., 1993). Constrained least-squares refinement was performed by X-PLOR (Brünger, 1992). After six cycles of refinement and solvent placement, the crystallographic *R* factors for the MbEtNC complex converged to the value of 15.9%. The coordinates and structure factors for the ethyl isocyanide complex of recombinant sperm whale myoglobin have been submitted to the Brookhaven Protein Data Bank under the access code 1TES.

RESULTS AND DISCUSSION

Time Courses and Rate Constants for the Oxidation of MbO_2. Figure 1A shows normalized time courses of the reactions of wild-type, Leu(B10) → Phe, and Leu(B10) → Trp MbO_2 with 5 μM NO at pH 7 and 20 °C. The original absorbance increases were measured at 409 nm and indicate the rapid appearance of aquometmyoglobin without any evidence for an intermediate. Identical normalized traces were observed at all wavelengths from 390 to 450 nm. Only

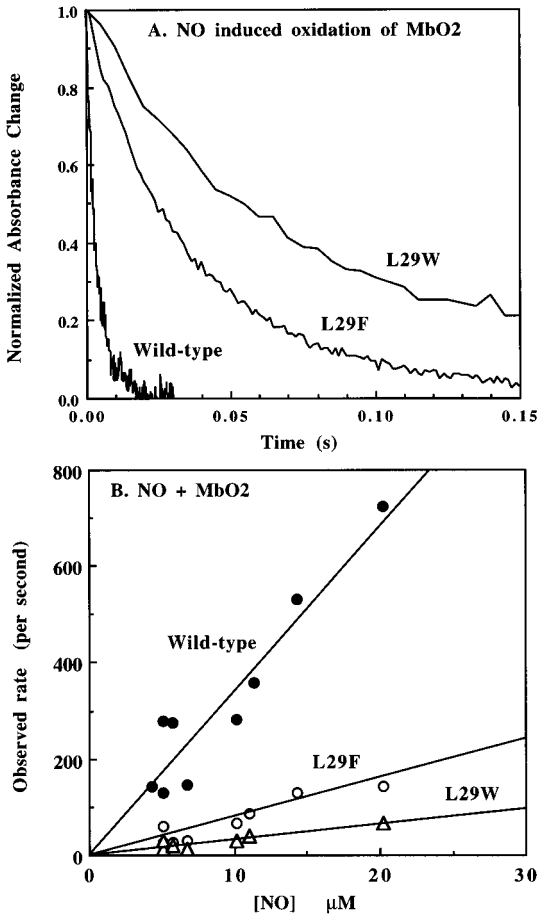

FIGURE 1: Kinetics of NO-induced oxidation of recombinant myoglobins at pH 7 and 20 °C. (A) Normalized time courses for the reaction of 0.5 μM wild-type, Leu(B10) → Phe(L29F), and Leu(B10) → Trp(L29W) recombinant sperm whale MbO_2 with 5 μM NO. (B) Plots of the k_{obs} versus [NO] for the reaction of NO with the oxymyoglobins listed in Table 1.

MbO_2 and met-Mb appear to be present during the reaction with little or no evidence for spectral intermediates on millisecond time scales. Minor slow changes can be observed on longer time scales at high [NO] and may be associated with either NO binding to newly formed aquometmyoglobin or side reactions due to peroxynitrite, nitrite, or nitrate.

All of the recombinant oxymyoglobins show time courses that can be fitted well to a single exponential expression with an offset. Plots of the pseudo first-order rate constants, k_{obs}, versus [NO] are linear with *y*-intercepts ≈ 0 (Figure 1B). The free oxygen concentration in some of the samples was varied from 63 to 625 μM without any effect on the observed rate. Thus, NO-induced oxidation of MbO_2 appears to be a simple bimolecular process as opposed to autooxidation which shows a complex dependence on $[O_2]$, the character of which changes with mutagenesis of distal pocket residues (Brantley et al., 1993).

As predicted by Doyle and Hoekstra (1981), the reaction of NO with wild-type oxymyoglobin is very rapid. The first-order dependence on [NO] and the lack of a limiting rate at high [NO] show that NO is not displacing bound O_2 but reacting directly with the bound ligand. The absolute values of the rate constants for NO-induced oxidation of wild-type MbO_2 are large and very similar to the bimolecular rate constant for NO binding to deoxy-Mb. As shown in Figure 2, there is a close 1:1 correlation between $k'_{ox,NO}$ and k'_{NO}-

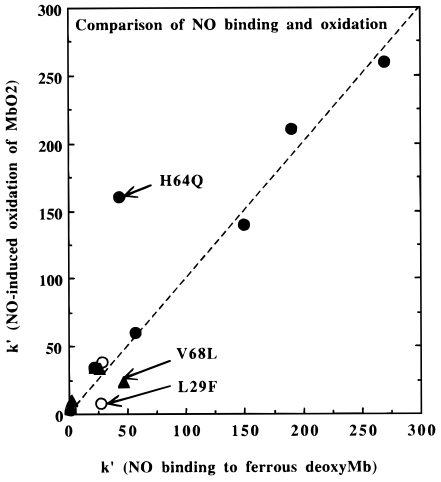

FIGURE 2: Comparison of the bimolecular rate constants for NO-induced oxidation with those for simple NO binding to recombinant myoglobins. $k'_{ox,NO}$ is plotted versus $k'_{NO}(Fe^{+2})$, showing an approximate 1:1 correspondence. The dashed line assumes $k'_{ox,NO} = k'_{NO}(Fe^{+2})$; the open circles, closed circles, and closed triangles represent data for position 29(B10), 64(E7), and 68(E11) mutants, respectively, taken from Table 1.

(Fe^{2+}) for 10 of the 13 recombinant myoglobins listed in Table 1. The exceptions are the Leu29(B10) → Phe, His64(E7) → Gln, and Val68(E11) → Leu mutations. Of these, only the Phe(B10) substitution produces a marked decrease in $k'_{ox,NO}$ without altering $k'_{NO}(Fe^{2+})$.

Mechanisms of NO Binding and Oxidation. Our view of NO binding to ferrous myoglobin is shown in the top panel of Figure 3 and was originally developed to explain O_2 and CO reactions [see Springer et al. (1994), Quillin et al. (1993, 1995), and Zhou et al. (1995)]. NO must first displace a water molecule in order to enter the distal pocket. Laser photolysis experiments, low-temperature X-ray crystallography, and molecular dynamics simulations have shown that noncovalently bound ligands reside in the space circumscribed by His64(E7), Leu29(B10), Val68(E11), and Ile107(G8) (Gibson et al., 1992; Schlichting et al., 1994; Quillin et al., 1995). Virtually every NO molecule that reaches the distal pocket reacts with the reduced iron atom before the gas has a chance to leave the protein. This high intrinsic chemical reactivity explains the low quantum yields and the large extent of geminate recombination observed in laser photolysis experiments with almost all MbNO and HbNO derivatives (Petrich et al., 1988; Gibson et al., 1992; Quillin et al., 1995). As a result, the rate-determining step for NO binding to deoxymyoglobin is ligand diffusion into the distal pocket. The primary pathway for this movement appears to be through a channel created by an outward rotation of the distal histidine and displacement of the water molecule hydrogen-bonded to this residue. The overall rate constant for NO binding to deoxy-Mb increases when His(E7) is replaced by nonpolar residues (Table 1; Quillin et al., 1993) and when His(E7) is allowed to rotate more freely by mutating Phe46(CD4) to smaller residues [e.g. $k'_{NO}(Fe^{2+}) = 63\ \mu M^{-1}\ s^{-1}$ for F46V Mb; Lai et al., 1995]. Aromatic substitutions at Val68(E11) decrease $k'_{NO}(Fe^{2+})$ markedly by sterically inhibiting access of NO to the noncovalent binding sites (Table 1; Quillin et al., 1995). A similar phenomenon occurs when Leu29(B10) is replaced by Phe (Gibson et al., 1992).

The correspondence between $k'_{ox,NO}$ and $k'_{NO}(Fe^{2+})$ suggests that the oxidative NO reaction occurs by a similar mechanism (bottom panel in Figure 3). In this case, transient disruption of the hydrogen bond between His(E7) and bound oxygen is probably required for the initial entry of NO into

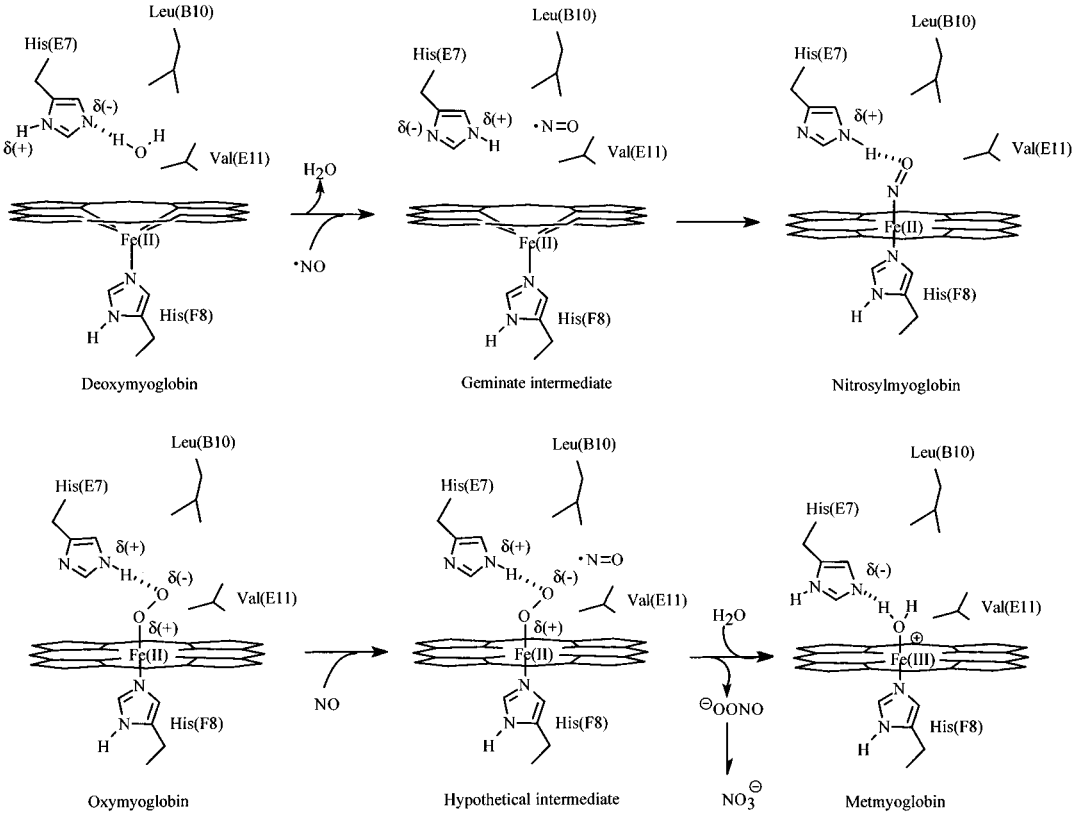

FIGURE 3: Proposed stereochemical mechanisms for NO binding to deoxy-Mb (upper panel) and NO-induced oxidation of MbO_2 (lower panel).

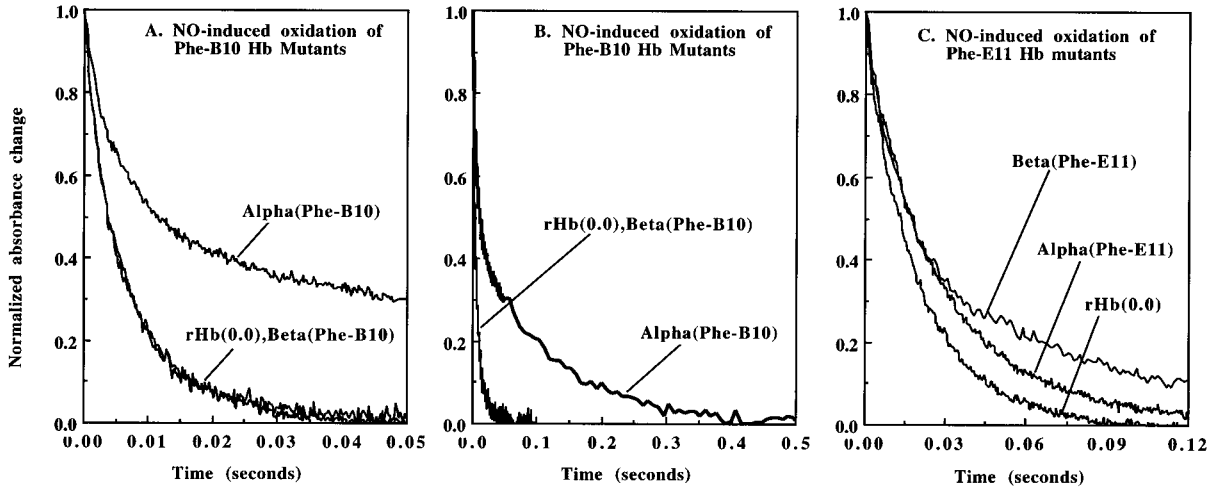

FIGURE 4: Time courses for NO-induced oxidation of recombinant hemoglobin, rHb(0.0). (A) The reactions of 0.5 μM rHb(0.0), α(Phe-B10)β(0.0) [labeled Alpha(Phe-B10)], and α(0.0)β(Phe-B10) [labeled Beta(Phe-B10)] HbO_2 with 2.5 μM NO. (B) The same data in panel A displayed on a longer time scale. (C) The reactions of 0.2 μM rHb(0.0), α(Phe-E11)β(0.0) [labeled Alpha(Phe-E11)], and α(0.0)β(Phe-E11) [labeled Beta(Phe-E11)] HbO_2 with 1 μM NO. The time courses for rHb(0.0) can be approximated by a single exponential expression, and the dependence on [NO] gives a value of $k'_{ox,NO} \approx 50\ \mu M^{-1}\ s^{-1}$ for both subunits. The time courses for the mutants were fitted to two exponential expressions, and the values of the bimolecular rate constants are as follows: 3 $\mu M^{-1}\ s^{-1}$, α(Phe-B10); 50 $\mu M^{-1}\ s^{-1}$, β(Phe-B10); 26 $\mu M^{-1}\ s^{-1}$, α(Phe-E11); and 11 $\mu M^{-1}\ s^{-1}$, β(Phe-E11). These rate constants apply to subunits in the R-state, $\alpha_1\beta_1$ dimer which is the predominant quaternary structure at low protein concentrations.

the distal pocket. Noncovalently bound NO then reacts rapidly with coordinated oxygen. This internal oxidation is analogous to the reaction of NO with superoxide anion which produces peroxynitrite and is diffusion-controlled, exhibiting a bimolecular rate constant of $\sim 7 \times 10^9\ M^{-1}\ s^{-1}$ (Huie & Padmaja, 1993). No intermediate met-Mb complex is seen, presumably because $OONO^-$ (or some other oxidation product) is quickly expelled from the protein due to its large size, polarity, and poor affinity for Fe^{3+}. Every NO molecule that enters the distal pocket reacts rapidly with the polarized $Fe-O_2$ complex, making the rate-limiting step diffusion into the distal pocket as is the case for simple NO binding.

In contrast to the ferrous reactions, NO binding to ferric myoglobin is limited by a completely different stereochemical process. In wild-type aquomet-Mb, water is coordinated to the iron atom, and as a result, the rate of ligand binding to this form of the protein is limited in part or in whole by the strength of the Fe^{3+}-OH_2 bond (Sharma et al., 1983, 1987; Brancaccio et al., 1994). The overall rate constants for NO binding to metmyoglobins with a distal histidine are $\sim$100 times smaller than the rate constants for NO binding to and oxidation of the corresponding ferrous proteins (Table 1). In addition, decreasing the size of the distal pocket by aromatic substitutions at the 29(B10) and 68(E11) positions causes much smaller decreases in $k'_{NO}(Fe^{3+})$ than those observed for $k'_{ox,NO}$ and $k'_{NO}(Fe^{2+})$. Only when His64 is replaced with apolar residues does the rate for NO binding to metmyoglobin approach that for binding to ferrous deoxymyoglobin. These dramatic increases in $k'_{NO}(Fe^{3+})$ are due to the loss of water coordination in these mutants and are similar to those reported for Asian elephant Mb and opossum Hb which have His(E7) $\rightarrow$ Gln substitutions (Sharma et al., 1983, 1987). Similar marked increases are observed for the rates of azide binding to these mutants (Brancaccio et al., 1994).

Selective Inhibition of NO Oxidation. The Leu29(B10) $\rightarrow$ Phe mutation causes little change in the association rate constants for the binding of either NO, O_2, or CO (Table 1; Carver et al., 1992). This lack of effect is a result of compensating events. In native and wild-type deoxymyoglobin, there is a water molecule hydrogen-bonded to the N_ϵ of His64 which inhibits the entry of ligands into the distal pocket (Figure 3; Rohlfs et al., 1990; Quillin et al., 1993). When Leu(B10) is replaced with Phe, the larger size of the benzyl side chain prevents water from hydrogen bonding to His64(E7) in deoxy-Mb (Quillin, 1994), and this absence of ordered internal water should enhance the rate of ligand entry into the mutant protein. However, the large phenylalanine side chain also inhibits the NO molecules from approaching the iron atom in the distal pocket. This effect is observed directly in nanosecond laser photolysis experiments as a reduction in the amplitude of geminate rebinding once the ligand has left the immediate vicinity of the iron atom in the Phe29(B10) mutant (Gibson et al., 1992). Thus, the favorable effect of displacing the distal pocket water molecule is offset by steric hindrance from the large aromatic side chain, and there is no net change in $k'_{NO}(Fe^{2+})$.

In the case of NO-induced oxidation of MbO_2, only the inhibitory effect of the benzyl side chain is observed since His64(E7) hydrogen bonds to bound oxygen in both wild-type protein and the Phe(B10) mutant. As a result, the Leu29(B10) $\rightarrow$ Phe mutation causes a 4-fold decrease in $k'_{ox,NO}$. When Leu(B10) is replaced with the even larger Trp residue, steric hindrance becomes the dominant factor, and both $k'_{NO}(Fe^{2+})$ and $k'_{ox,NO}$ decrease markedly (Figure 1, Table 1).

Effects of Phe(B10) and Phe(E11) Mutations on NO-Induced Oxidation of Recombinant Hemoglobin. On the basis of the myoglobin results in Table 1, Leu(B10) $\rightarrow$ Phe and Val(E11) $\rightarrow$ Phe mutations are good candidates for incorporating resistance to NO-induced oxidation into recombinant hemoglobin. The results of our first attempts to engineer the active sites of the α and β subunits of human hemoglobin are shown in Figure 4. The Leu(B10) $\rightarrow$ Phe replacement causes a dramatic 17-fold decrease in the rate constant for NO-induced oxidation of α subunits, from $\sim$50 to 3 $\mu M^{-1}\ s^{-1}$. In contrast, this mutation produces little or no effect on the reaction of NO with β subunits (Figure

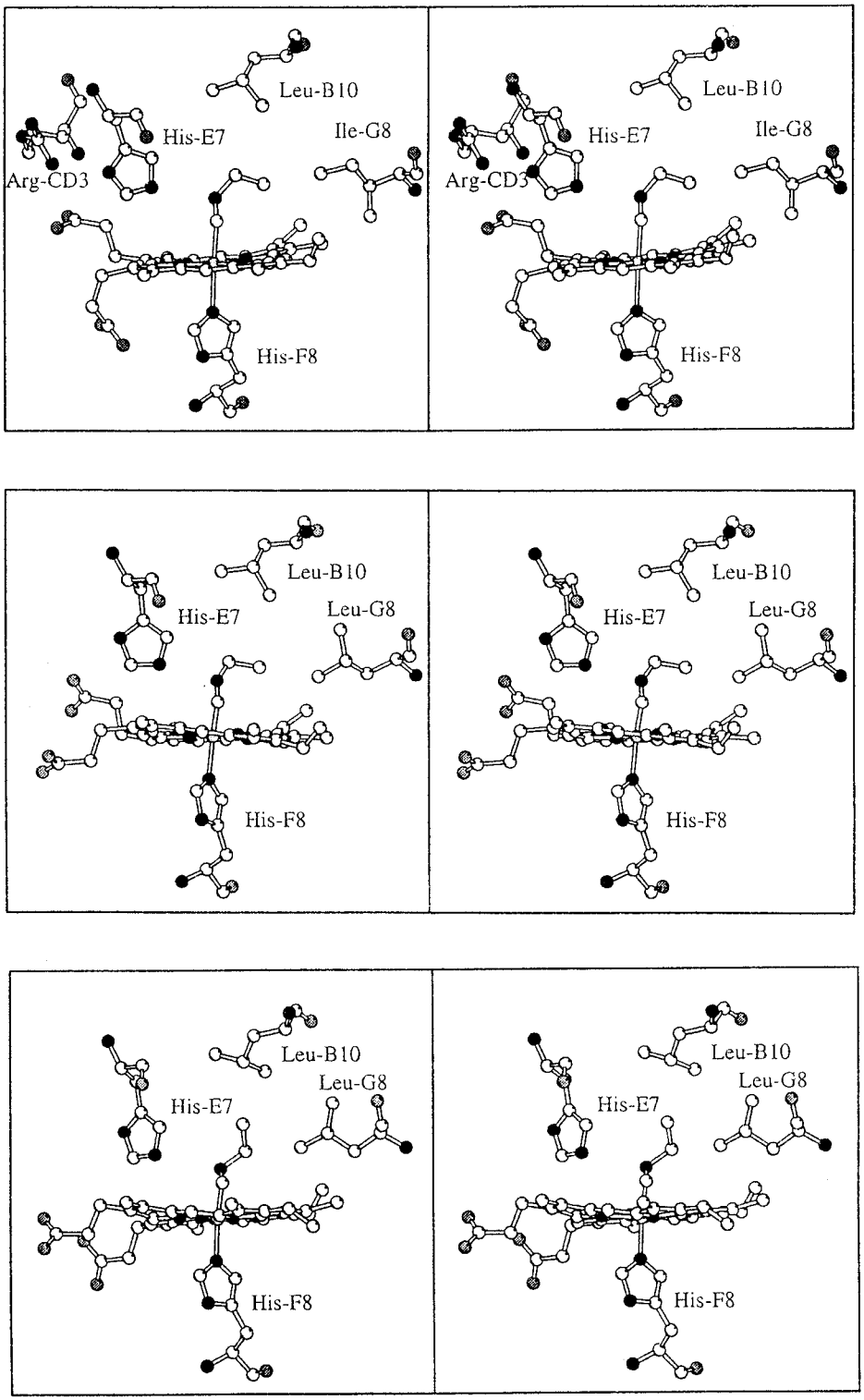

FIGURE 5: Stereodrawings of the crystal structures of recombinant sperm whale myoglobin (upper panel) in the *P*6 crystal form and of the α (middle panel) and β (lower panel) subunits within the ethyl isocyanide complex of native human hemoglobin. The *P*6 wild-type myoglobin structure is similar to that reported for the ethyl isocyanide complex of native sperm whale myoglobin, except for the position of the distal histidine which is in the "up" position in the $P2_1$ form (Johnson et al., 1989; PDB accession code 2MYE). The hemoglobin structures were taken from Johnson (1993; PDB accession code 2HBC).

4A,B). In the case of the Val(E11) → Phe mutation, there is a 5-fold decrease in $k'_{ox,NO}$ for β subunits, from ~50 to 11 μM^{-1} s^{-1}, whereas the α subunit rate constant decreases only 2-fold (Figure 4C).

The marked differences between the effects of the Phe-(B10) substitution on the α and β subunits are readily interpreted from the structure of the ethyl isocyanide complex of native human hemoglobin (Figure 5; Johnson, 1993). Bound ethyl isocyanide serves as a structural model for the transition state of the NO-induced oxidation reaction (Figure 5). Fe═C═N mimics the iron−dioxygen complex, and the ethyl side chain represents noncovalently bound NO in a position to contact the second bound O atom. Leu-B10 sterically limits the space adjacent to the ligand binding site in both myoglobin (Figure 5, upper panel) and α subunits (middle panel), and bound ethyl isocyanide is markedly

"bent" in both of these proteins. In contrast, the Leu(B10) side chain in β subunits is able to move out of the way, allowing bound ethyl isocyanide to adopt a more upright conformation (Figure 5, lower panel). The flexibility of Leu(B10) in β chains explains why isocyanides, O_2, and NO react more rapidly with this subunit than with α subunits (Mathews & Olson, 1994). Presumably, a similar phenomenon explains the lack of effect of the Leu(B10) → Phe mutation on NO-induced oxidation of β subunits. The large benzyl side chain can move out of the way of incoming NO in β subunits, whereas large residues at the B10 position severely restrict access to bound O_2 in the distal pocket of α subunits.

The differential effect of the Val(E11) → Phe mutation can be explained by the proximity of the E11 residue to the bound ligand. The distances between $C_{\gamma 2}$ of Val(E11) and the alkyl carbon atoms of bound ethyl isocyanide are 3.5−3.7 Å in β subunits and Mb and 4.3−4.8 Å in α subunits (Johnson, 1993). Presumably, the Phe(E11) side chain is also closer to the iron atom in mutant β subunits, inhibiting both noncovalent NO binding and its approach to bound O_2. However, the differential effect of the Phe(E11) mutation on the α and β subunits is small compared to that for the Phe(B10) substitution. A more detailed interpretation will require crystal structures for a complete set of mutant hemoglobins and kinetic studies with stabilized hemoglobin tetramers.

Conclusions and Future Strategies. The results in Figure 4 demonstrate the power of using stereochemical and biophysical mechanisms for the rational design of protein-based O_2 carriers. Our goal is to construct an active site that is resistant to both auto- and NO-induced oxidation but still has moderate O_2 affinity and large association and dissociation rate constants for efficient transport *in vivo* [see Lemon et al. (1987), Olson (1994), and Vandegriff and Winslow (1995)]. NO-induced oxidation of MbO_2 occurs by a process analogous to that observed for simple NO binding to the deoxy forms of these proteins. The rate-limiting step in both cases is ligand diffusion into the distal pocket which is followed by rapid reaction either with the superoxide form of bound oxygen or with the Fe^{2+} atom. This mechanism provides a strategy for inhibiting the oxidative reaction by filling the space adjacent to the bound O_2 with large aromatic residues. A similar approach has been adopted by Olson and co-workers to inhibit autooxidation (Brantley et al., 1993; Olson, 1994; Zhao et al., 1995).

The results in Figure 4 also show the limitations of using Mb as a prototype for rational mutagenesis of hemoglobin. The inhibitory effect of the Leu(B10) → Phe mutation in myoglobin is exaggerated in α subunits but is not seen at all in β subunits. Thus, effects seen in Mb do not always correlate directly with those observed in the individual subunits of hemoglobin. However, the general strategy of filling the free space in the distal pocket adjacent to bound O_2 does work to reduce the rate of NO-induced oxidation in both subunits.

The structural factors that govern ligand binding and oxidation are often very similar (Olson, 1994). Our mutagenesis and structural work suggests that O_2 affinity is regulated more strongly by hydrogen bonding to the distal histidine than by the free volume and extent of hindrance in the distal pocket (Quillin et al., 1993). In contrast, the latter properties appear to play a more important role in governing the rate of NO-induced oxidation (Table 1). Thus, multiple mutations, generated either rationally or randomly, should allow selective inhibition of unfavorable oxidative reactions.

REFERENCES

Alayash, A. I., & Cashon, R. E. (1994) *Ann. N.Y. Acad. Sci. 8*, 738−781.

Alayash, A. I., Fratantoni, J. C., Bonaventura, C., Bonaventura, J., & Cashon, R. E. (1993) *Arch. Biochem. Biophys. 303*, 332−338.

Brancaccio, A., Cutruzzola, F., Travaglini Allocatelli, C., Brunori, M., Smerdon, S. J., Wilkinson, A. J., Dou, Y., Keenan, D., Ikeda-Saito, M., Brantley, R. E., Jr., & Olson, J. S. (1994) *J. Biol. Chem. 269*, 13843−13853.

Brantley, R. E., Jr., Smerdon, S. J., Wilkinson, A. J., Singleton, E. W., & Olson, J. S. (1993) *J. Biol. Chem. 268*, 6995−7010.

Brünger, A. (1992) *X-PLOR 3.1 Manual*, Yale University Press, New Haven.

Carver, T. E., Brantley, R. E., Jr., Singleton, E. W., Arduini, R. M., Quillin, M. L., Phillips, G. N., Jr., & Olson, J. S. (1992) *J. Biol. Chem. 267*, 14443−14450.

Doyle, M. P., & Hoekstra, J. W. (1981) *J. Inorg. Biochem. 14*, 351−358.

Egeberg, K. D., Springer, B. A., Sligar, S. G., Carver, T. E., Rohlfs, R. J., & Olson, J. S. (1990) *J. Biol. Chem. 265*, 11788−11795.

Gibson, Q. H., Regan, R., Elber, R., Olson, J. S., & Carver, T. E. (1992) *J. Biol. Chem. 267*, 22022−22034.

Hargrove, M. S., Singleton, E. W., Quillin, M. L., Ortiz, L. A., Phillips, G. N., Jr., & Olson, J. S. (1994) *J. Biol. Chem. 269*, 4207−4214.

Hess, J. R., MacDonald, V. W., & Brinkley, W. W. (1993) *J. Appl. Physiol. 74*, 1769−1778.

Hoffman, S. J., Looker, D. L., Roehrich, J. M., Cozart, P. E., Durfee, S. L., Tedesco, J. L., & Stetler, G. L. (1990) *Proc. Natl. Acad. Sci. U.S.A. 87*, 8521−8525.

Huie, R. E., & Padmaja, S. (1993) *Free Radical Res. Commun. 18*, 195−199.

Hurshman, A. R., & Marletta, M. A. (1995) *Biochemistry 34*, 5627−5634.

Ignarro, L. J. (1990) *Annu. Rev. Pharmacol. Toxicol. 30*, 535−560.

Innis, M. A., Gelfand, D. H., Sninsky, J. J., & White, T. J., Eds. (1990) *PCR Protocols: A Guide to Methods and Applications*, Academic Press, San Diego.

Johnson, K. A. (1993) Ph.D. Dissertation, Rice University, Houston, TX.

Johnson, K. A., Olson, J. S., & Phillips, G. N., Jr. (1989) *J. Mol. Biol. 207*, 459−463.

Kharitonov, V. G., Sundquist, A. R., & Sharma, V. S. (1994) *J. Biol. Chem. 269*, 5881−5883.

Komiyama, N., Shih, D., Looker, D., Tame, J., & Nagai, K. (1991) *Nature 352*, 349−351.

Kosaka, H., Sawai, Y., Sakaguchi, H., Kumura, E., Harada, N., Watanabe, M., & Shiga, T. (1994) *Am. J. Physiol. 266*, C1400−C1405.

Lai, H. H., Li, T., Lyons, D. S., Phillips, G. N., Jr., & Olson, J. S. (1995) *Proteins: Struct., Funct., Genet. 22*, 322−339.

Lee, R., Neya, K., Svizzero, T. A., & Vlahakes, G. J. (1995) *J. Appl. Physiol. 79*, 236−242.

Lemon, D. D., Nair, P. K., Boland, E. J., Olson, J. S., & Hellums, J. D. (1987) *J. Appl. Physiol. 62*, 798−806.

Lieberthal, W., Wolf, E. F., Merrill, E. W., Levinsky, N. G., & Valeri, C. R. (1987) *Life Sci. 41*, 2525−2533.

Looker, D., Abbot-Brown, D., Cozart, P., Durfee, S., Hoffman, S., Mathews, A. J., Miller-Roehrich, J., Shoemaker, S., Trimble, S., Fermi, G., Komiyama, N. H., Nagai, K., & Stetler, G. (1992) *Nature 356*, 258−260.

Marletta, M. A. (1993) *J. Biol. Chem. 268*, 12231−12234.

Mathews, A. J., & Olson, J. S. (1994) *Methods Enzymol. 232*, 363−386.

Mathews, A. J., Rohlfs, R. J., Olson, J. S., Tame, J., Renaud, J.-P., & Nagai, K. (1989) *J. Biol. Chem. 264*, 16573−16583.

Moncada, S., Palmer, R. M. J., & Higgs, E. A. (1991) *Pharmacol. Rev. 43*, 109−142.

Nagai, K., Luisi, B., Shih, D., Miyazaki, G., Imai, K., Poyart, C., De Young, A., Kwiatkowsky, L., Noble, R. W., Lin, S.-H., & Yu, N.-T. (1987) *Nature 329*, 858−860.
Olson, J. S. (1994) *Biomater., Artif. Cells, Immobilization Biotechnol. 22*, 429−441.
Petrich, J. W., Poyart, C., & Martin, J. L. (1988) *Biochemistry 27*, 4049−4060.
Phillips, G. N., Jr., Arduini, R. M., Springer, B. A., & Sligar S. G. (1990) *Proteins: Struct., Funct., Genet. 7*, 358−365.
Quillin, M. L. (1994) Ph.D. Dissertation, William Marsh Rice University, Houston, TX.
Quillin, M. L., Arduini, R. M., Olson, J. S., & Phillips, G. N., Jr. (1993) *J. Mol. Biol. 234*, 140−155.
Quillin, M. L., Li, T., Olson, J. S., Phillips, G. N., Jr., Dou, Y., Ikeda-Saito, M., Elber, R., Li, H., Regan, R., & Gibson, Q. H. (1995) *J. Mol. Biol. 245*, 416−436.
Rohlfs, R. J., Mathews, A. J., Carver, T. E., Olson, J. S., Springer, B. A., Egeberg, K. D., & Sligar, S. G. (1990) *J. Biol. Chem. 265*, 3168−3176.
Schlichting, I., Berendzen, J., Phillips, G. N., Jr., & Sweet, R. M. (1994) *Nature 371*, 808−812.
Sharma, V. S., Isaacson, R. A., John, M. E., Waterman, M. R., & Chevion, M. (1983) *Biochemistry 22*, 3897−3902.
Sharma, V. S., Traylor, T. G., Gardiner, R., & Mizukami, H. (1987) *Biochemistry 26*, 3837−3843.
Snyder, S. H., & Bredt, D. S. (1992) *Sci. Am.* (May), 68−77.
Springer, B. A., & Sligar, S. G. (1987) *Proc. Natl. Acad. Sci. U.S.A. 84*, 8961−8965.
Springer, B. A., Egeberg, K. D., Sligar, S. G., Rohlfs, R. J., Mathews, A. J., & Olson, J. S. (1989) *J. Biol. Chem. 264*, 3057−3060.
Springer, B. A., Sligar, S. G., Olson, J. S., & Phillips, G. N., Jr. (1994) *Chem. Rev. 94*, 699−714.
Vandegriff, K. D. (1992) *Biotechnol. Genet. Eng. Rev. 10*, 403−453.
Vandegriff, K. D. (1995) in *Blood Substitutes: Physiological Basis of Efficacy* (Winslow, R. M., Vandegriff, K. D., & Intaglietta, M., Eds.) pp 105−131, Birkhauser, Boston.
Vandegriff, K. D., & Winslow, R. M. (1995) in *Blood Substitutes: Physiological Basis of Efficacy* (Winslow, R. M., Vandegriff, K. D., & Intaglietta, M., Eds.) pp 143−154, Birkhauser, Boston.
Zhao, X., Vyas, K., Nguyen, B. D., Rajarathnam, K., La Mar, G. N., Ling, J., Bocian, D. F., Li, T., Phillips, G. N., Jr., Eich, R. F., & Olson, J. S. (1995) *J. Biol. Chem. 270*, 20763−20774.

BI960442G